

## Electronic structure of alkali-metal overlayers on the semi-infinite jellium surface

H. Ishida

*Institute for Solid State Physics, University of Tokyo, Roppongi, Minato-ku, Tokyo 106, Japan*

(Received 14 November 1988)

A self-consistent electronic-structure calculation of alkali-metal overlayers on the semi-infinite jellium surface is performed within the local-density-functional theory combined with the embedding-potential method. The results obtained confirm that the adatom charge state is very insensitive to coverage ( $\Theta$ ), and also that the hybridization between adatom and substrate states plays an important role in the adatom-induced dipole and its  $\Theta$  dependence.

Alkali-metal adsorption on metal surfaces had been believed to be one of the few chemisorption systems whose electronic properties could be understood well with a simplified model.<sup>1</sup> Indeed, the ionic-to-neutral change of adatoms with increasing coverage ( $\Theta$ ), originally proposed by Gurney<sup>2</sup> and supported by model calculations<sup>3-5</sup> based on the Newns-Anderson (NA) Hamiltonian,<sup>6,7</sup> had been accepted as a basic concept in this field for a long time. Very recently, Ishida,<sup>8</sup> and Ishida and Terakura<sup>9</sup> reported details of the electronic structure of alkali-metal overlayers on the jellium and Al(001) surfaces, respectively. It was shown that the depolarization field, a central quantity which shifts down adatom resonances and neutralizes adatoms at higher  $\Theta$ , is virtually absent, and consequently, the adatom-charge state is remarkably independent of  $\Theta$ . This was not in accord with the existing simplified view.

The drawback of these later calculations was in the use of a *finite* slab as substrate, enforced to keep translational symmetry in the surface normal direction, which resulted in spiky sharp peaks in the calculated adatom density of states (DOS) at low  $\Theta$ , thus making a precise location of adatom resonances somewhat ambiguous. In this paper, we perform a self-consistent electronic-structure calculation of alkali-metal overlayers on a truly *semi-infinite* jellium and remove all the uncertainties involved in the slab

calculations. Although the calculational method is quite different, the current work corresponds to an extension to the finite- $\Theta$  regime of the well-known work of Lang and Williams<sup>10,11</sup> on single-atom adsorption on jellium.

The calculation is done within the local-density-functional theory combined with the embedding method of Inglesfield.<sup>12</sup> Figure 1 depicts the geometry used in the present calculation.<sup>13</sup> Only the embedded region with  $b_1 \leq z \leq b_2$  is treated explicitly, and the effects of the bulk jellium ( $z < b_1$ ) and vacuum ( $z > b_2$ ) are expressed in terms of the embedding potentials which act on two embedding surfaces at  $z = b_1$  and  $b_2$ . To describe electron wave functions in the embedded region as well as their logarithmic derivatives at the boundaries, the Green function  $G(\mathbf{r}, \mathbf{r}', \varepsilon, \Theta) = \langle \mathbf{r} | [\varepsilon + i\delta - H(\Theta)]^{-1} | \mathbf{r}' \rangle$  is expanded by the nonorthogonal basis set,

$$\phi_{\mathbf{k}+\mathbf{G},n}(\mathbf{r}) = \left[ \frac{2}{Sl} \right]^{1/2} \exp[i(\mathbf{k}+\mathbf{G}) \cdot \mathbf{x}] \sin(k_n z), \quad (b_1 \leq z \leq b_2), \quad (1)$$

where  $k_n = n\pi/l$  ( $n > 0$ ),  $S$  is the area of the surface, and  $\mathbf{k}$  and  $\mathbf{G}$  denote the two-dimensional wave vector and reciprocal lattice vector, respectively. The matrix element of the energy-dependent embedding potential at  $z = b_1$  is given as

$$H_{b_1}(\mathbf{k}+\mathbf{G},n;\mathbf{k}+\mathbf{G}',n') = \frac{1}{l} [(\mathbf{k}+\mathbf{G})^2 - 2\varepsilon]^{1/2} \sin(k_n b_1) \sin(k_{n'} b_1) \delta_{\mathbf{G},\mathbf{G}'}, \quad (2)$$

where the energy  $\varepsilon$  is measured from the bottom of the jellium band, and the imaginary part of  $H_{b_1}$  is chosen positive if  $2\varepsilon > (\mathbf{k}+\mathbf{G})^2$  (through the paper, we use the atomic units,  $m = e = \hbar = 1$ , where the units of length and energy are 0.529 Å and 27.2 eV, respectively). The matrix element of the embedding potential at  $z = b_2$  is obtained by replacing  $\varepsilon$  in Eq. (2) by  $\varepsilon - \varepsilon_{\text{vac}}$ , and  $b_1$  by  $b_2$ , where  $\varepsilon_{\text{vac}}$  is the potential barrier at the vacuum which should be determined self-consistently. The latter embedding surface was not considered in the recent formulation of Inglesfield and Benesh,<sup>14,15</sup> but is necessary in reproducing energy spectra above the vacuum level. The other matrix elements of the Hamiltonian are calculated in a similar way as in standard slab calculations. We use the non-

local norm-conserving pseudopotential<sup>16</sup> for alkali-metal adatoms.

In this paper, we show the results for Na overlayers on the jellium with  $r_s = 2.1$  a.u., which corresponds to the bulk Al electron density. The overlayer is assumed to form a square lattice with lattice constant  $a$ , and the distance between the jellium edge and Na atom is set equal to 3 a.u. irrespective of  $\Theta$ .<sup>17</sup> Just for the sake of convenience, we define the coverage corresponding to  $a = 8$  a.u. as  $\Theta = 1$ . The cut-off energy for the basis function (1) is 5 Ry, and self-consistency is assumed when the difference between the input and output potential barriers at the vacuum becomes less than 0.15 eV. The calculated work function shows a well-known characteristic  $\Theta$  dependence:

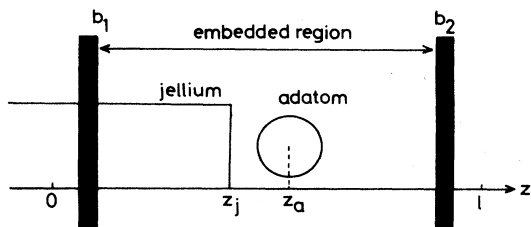


FIG. 1. The alkali-metal overlayer on the semi-infinite jellium. Only the embedded region with  $b_1 \leq z \leq b_2$  is treated explicitly in the self-consistent calculation.

an initial rapid lowering from that of the jellium, 3.8 eV, which is followed by a minimum, 2.3 eV at  $\Theta \cong \frac{1}{2}$  ( $a = 11.31$  a.u.), and a subsequent small rise to 2.8 eV at  $\Theta = 1$ . The adatom dipole  $d(\Theta)$  at  $\Theta = \frac{1}{5}$  ( $a = 17.89$  a.u.), the lowest  $\Theta$  in the present calculation, is nearly five times as large as that at  $\Theta = 1$ . Since quantities such as the electron charge density and work function to which all the states below the Fermi level  $\epsilon_F$  contribute are close to those in the previous slab calculation,<sup>8</sup> we focus here on the adatom-electronic state as a function of the one-electron energy.

The full curves in Fig. 2 show the calculated total DOS of Na,  $\rho_a(\epsilon, \Theta)$  defined by

$$\rho_a(\epsilon, \Theta) = -\frac{1}{\pi} \int d\mathbf{r} [\text{Im}G(\mathbf{r}, \mathbf{r}, \epsilon, \Theta) - \text{Im}G(\mathbf{r}, \mathbf{r}, \epsilon, \Theta = 0)], \quad (3)$$

where the integration is done within a Na atomic sphere with a radius  $R$  equal to 3.8 a.u.<sup>18</sup> Qualitative features of the results are insensitive to small differences of  $R$ . The long-dashed, short-dashed, and dot-dashed curves in Fig. 2 show the decomposition of  $\rho_a(\epsilon, \Theta)$  into the  $s$ ,  $p_z$ , and  $p_x$  ( $p_y$ ) partial DOS of Na, respectively. The calculated  $\rho_a(\epsilon, \Theta)$  at  $\Theta = \frac{1}{5}$  is very close to that given by Lang and Williams<sup>11</sup> in the study of single Na atom chemisorption on jellium, indicating that direct interaction among adatoms is negligibly small at  $\Theta = \frac{1}{5}$ . The main peak in  $\rho_a(\epsilon, \Theta) \sim 1$  eV above  $\epsilon_F$  has been believed to be evidence of the almost empty Na  $3s$  state at low  $\Theta$ . However, Fig. 2(a) shows that it is actually a hybridized state of Na  $3s$  and  $3p_z$  rather than pure Na  $3s$ . Due to the strong adatom-substrate interaction, the two components do not form separated peaks. As will be shown later, the peak corresponds to an antibonding state with regard to the adatom-substrate bonding which strongly polarizes to the vacuum side of Na. On the other hand, the second peak located  $\sim 2.5$  eV above  $\epsilon_F$  is mainly due to the Na  $3p_x$  and  $p_y$  resonances. They have longer tails than Na  $3p_z$  and give some contribution to the occupied part of  $\rho_a(\epsilon, \Theta)$ . Figure 2(b) shows the total and partial DOS of Na at  $\Theta = \frac{1}{2}$  which is close to the work function minimum. It is seen that, because of increased (but still small) overlapping of neighboring adatom orbitals, the peaks in  $\rho_a(\epsilon, \Theta)$  are a little broader than those at  $\Theta = \frac{1}{5}$ . However, it is important that the deviation of  $\rho_a(\epsilon, \Theta)$  from the corresponding one in the limit of  $\Theta \rightarrow 0$  is a

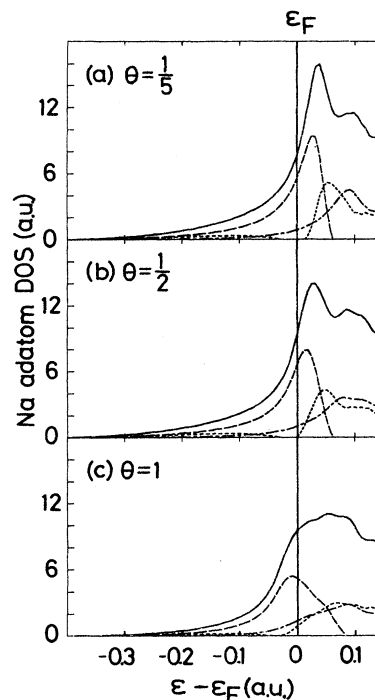


FIG. 2. The calculated total and partial state densities of Na on the jellium with  $r_s = 2.1$  a.u. at  $\Theta = \frac{1}{5}$ ,  $\frac{1}{2}$ , and 1. The total,  $s$ ,  $p_z$ , and  $p_x$  ( $p_y$ ) state densities are shown by solid, long-dashed, short-dashed, and dot-dashed curves, respectively.

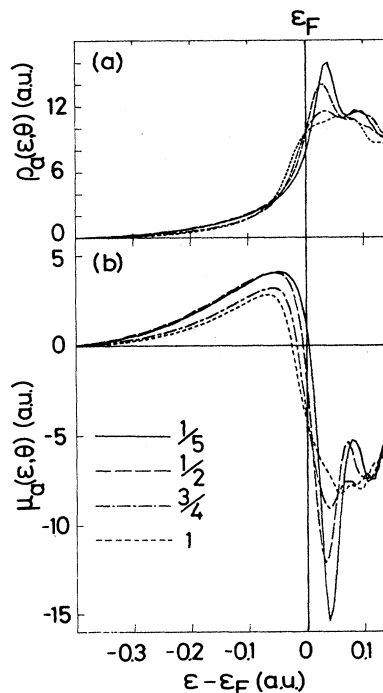


FIG. 3. The calculated total DOS  $\rho_a(\epsilon, \Theta)$  and induced dipole density  $\mu_d(\epsilon, \Theta)$  of a Na adatom on the jellium with  $r_s = 2.1$  a.u. The solid, long-dashed, dot-dashed, and short-dashed curves correspond to  $\Theta = \frac{1}{5}$ ,  $\frac{1}{2}$ ,  $\frac{3}{4}$ , and 1, respectively.

minor one as compared with the large lowering of the electrostatic potential in the vacuum, which amounts to 1.5 eV at  $\Theta = \frac{1}{2}$ .<sup>19</sup> This reflects the fact that the adatom potential within an atomic sphere is actually very insensitive to  $\Theta$  by virtue of efficient screening of the high-density metal substrate, as was clarified in the previous slab calculations.<sup>8,9</sup> The depolarization shift of resonant levels based on the classical point-charge-transfer model<sup>3-5</sup> is overestimated. On the other hand, large changes in  $\rho_a(\epsilon, \Theta)$  appear between  $\Theta = \frac{1}{2}$  and 1, where the direct interaction among neighboring adatoms rapidly increases. It is seen that the main peak above  $\epsilon_F$  found at lower  $\Theta$  entirely disappears at  $\Theta = 1$ , corresponding to formation of the broad Na valence bands. Simultaneously, the tail of  $\rho_a(\epsilon, \Theta)$  in the low-energy side below  $\epsilon_F$  shrinks to some extent as a result of the weaker adatom-substrate interaction at higher  $\Theta$  which follows the increased Na-Na interaction.

Figure 3(a) summarizes the  $\Theta$  dependence of  $\rho_a(\epsilon, \Theta)$ . In spite of the rapid decrease of  $d(\Theta)$  with increasing  $\Theta$ , the Na charge state  $n_a(\Theta)$ , evaluated by integrating  $\rho_a(\epsilon, \Theta)$  up to  $\epsilon_F$ , is quite insensitive to  $\Theta$ : the increase in  $\rho_a(\epsilon, \Theta)$  near  $\epsilon_F$  with increasing  $\Theta$  is mostly canceled by its decrease in the tail region. Of course, the Friedel sum rule ensures  $n_a(\Theta) = 1$  irrespective of  $\Theta$  if the integration in Eq. (3) is done in all the space. However, what is important here is that  $n_a(\Theta)$  does not depend on  $\Theta$  regardless of the choice of  $R$ . Moreover,  $n_a(\Theta)$  is a little larger than  $n_a^{\text{iso}}(\Theta)$  calculated for isolated Na layers irrespective of  $\Theta$ , implying that the adatom region is essentially neutral. In previous theories<sup>3-5</sup> based on the NA Hamiltonian, the adatom dipole was evaluated as  $d(\Theta) = D[1 - n_a(\Theta)]$ . Therefore, the large change in  $n_a(\Theta)$  with  $\Theta$  was prerequisite to the rapid decrease of  $d(\Theta)$ . However,  $d(\Theta)$  should additionally include the polarization term due to hybridization of the adatom and substrate states, and should be written as

$$d(\Theta) = D \left[ 1 - \sum_a \langle C_a^\dagger C_a \rangle \right] + \sum_{a,b} \mu_{ab} \langle C_a^\dagger C_b \rangle + \text{c.c.}, \quad (4)$$

where  $a$  and  $b$  denote the adatom and substrate states, and  $D$  and  $\mu_{ab}$  are dipole matrix elements.<sup>8</sup> The first term disappears when adatoms are neutral, while the second becomes the largest when  $\epsilon_F$  is located at the bonding-antibonding boundary with respect to the adatom-substrate bonding.

In order to examine the origin of  $d(\Theta)$  as well as the nature of adatom-substrate bonding, we calculate the induced dipole density  $\mu_a(\epsilon, \Theta)$  defined by

$$\mu_a(\epsilon, \Theta) = -\frac{1}{\pi} \int d\mathbf{r} (z - z_a) [\text{Im}G(\mathbf{r}, \mathbf{r}, \epsilon, \Theta) - \text{Im}G(\mathbf{r}, \mathbf{r}, \epsilon, \Theta = 0)], \quad (5)$$

where  $z_a$  is the  $z$  coordinate of a Na atom, and the integration is done in the same atomic sphere as for  $\rho_a(\epsilon, \Theta)$ . The induced dipole within the sphere is obtained by integrating  $\mu_a(\epsilon, \Theta)$  up to  $\epsilon_F$ . The calculated  $\mu_a(\epsilon, \Theta)$  is shown in Fig. 3(b), where its positive sign designates an inward polarization of electron wave functions which leads to the build up of the charge density in the interface, and thus work function lowering. Figure 3(b) shows that the main peak in  $\rho_a(\epsilon, \Theta)$  at lower  $\Theta$  is an antibonding state whose wave function strongly polarizes toward the vacuum side of Na as stated before.<sup>20</sup> At  $\Theta = \frac{1}{2}$ , the bonding-antibonding boundary in  $\mu_a(\epsilon, \Theta)$  coincides well with  $\epsilon_F$ , suggesting the formation of a metallic adatom-substrate bond even at low  $\Theta$  by the maximum use of bonding states, as well as the important role of the second term of Eq. (4). It should be noted that the positive  $\mu_a(\epsilon, \Theta)$  below  $\epsilon_F$  comes from the mixing of Na  $3s$  and substrate states rather than the intra-atomic polarization ( $3s-3p_z$  mixing), since the Na  $3p_z$  state is located above  $\epsilon_F$  at  $\Theta = \frac{1}{2}$ . With increasing  $\Theta$ , the inward polarization of electron wave functions below  $\epsilon_F$  becomes smaller, which results in a weaker adatom-substrate bonding and smaller  $d(\Theta)$  at higher  $\Theta$ . At the same time, one notices a small shift down of the bonding-antibonding boundary in  $\mu_a(\epsilon, \Theta)$  with increasing  $\Theta$  which accelerates the decrease of  $d(\Theta)$ . As is seen from Fig. 2, the boundary roughly corresponds to the lower edge of the Na  $3p_z$  band. Therefore, the partial filling of the strong antibonding state, which is above  $\epsilon_F$  at low  $\Theta$ , owing to the increased Na valence bandwidth may also play an important role in the rapid decrease of  $d(\Theta)$  and weakening of the adatom-substrate bond with increasing  $\Theta$ .

In conclusion, we performed the first self-consistent electronic structure calculation of alkali-metal overlayers on the *semi-infinite* jellium. The results confirmed the absence of large depolarization shifts of adatom states as well as the important role of the hybridization between adatom and substrate valence states in the induced dipole moment. The present calculational scheme may be applicable to many other interesting chemisorption systems whose substrate can be modeled by jellium.

The author is grateful to Professor K. Terakura and Professor M. Nakayama for valuable discussions. This work is partially supported by a Grant-in-Aid for Scientific Research on Priority Areas by the Ministry of Education, Science and Culture. The numerical computation was done at the Computer Centers of University of Tokyo, Institute for Molecular Science and Institute for Solid State Physics.

<sup>1</sup>For example, J. P. Muscat and D. M. Newns, *Prog. Surf. Sci.* **9**, 1 (1978); N. D. Lang, in *Theory of the Inhomogeneous Electron Gas*, edited by S. Lundqvist and N. H. March (Plenum, New York, 1983).

<sup>2</sup>R. W. Gurney, *Phys. Rev.* **47**, 479 (1935).

<sup>3</sup>J. P. Muscat and D. M. Newns, *Solid State Commun.* **11**, 737

(1972); *J. Phys. C* **7**, 2630 (1974).

<sup>4</sup>J. P. Muscat and I. P. Batra, *Phys. Rev. B* **34**, 2889 (1986).

<sup>5</sup>H. Ishida, N. Shima, and M. Tsukada, *Surf. Sci.* **158**, 438 (1985).

<sup>6</sup>D. M. Newns, *Phys. Rev.* **178**, 1123 (1969).

<sup>7</sup>P. W. Anderson, *Phys. Rev.* **124**, 41 (1961).

- <sup>8</sup>H. Ishida, Phys. Rev. B **38**, 8006 (1988). See also, H. Ishida and K. Terakura, Phys. Rev. B **36**, 4510 (1987).
- <sup>9</sup>H. Ishida and K. Terakura, Phys. Rev. B **38**, 5752 (1988).
- <sup>10</sup>N. D. Lang and A. R. Williams, Phys. Rev. B **18**, 616 (1978).
- <sup>11</sup>N. D. Lang and A. R. Williams, Phys. Rev. B **16**, 2408 (1977).
- <sup>12</sup>J. E. Inglesfield, J. Phys. C **14**, 3795 (1981).
- <sup>13</sup>In the present work  $b_1$ ,  $z_j$ ,  $z_a$ ,  $b_2$ , and  $l$  are chosen as 2, 8, 11, 20, and 22 a.u., respectively.
- <sup>14</sup>G. A. Benesh and J. E. Inglesfield, J. Phys. C **17**, 1595 (1984).
- <sup>15</sup>J. E. Inglesfield and G. A. Benesh, Phys. Rev. B **37**, 6682 (1988).
- <sup>16</sup>G. B. Bachelet, D. R. Hamann, and M. Schlüter, Phys. Rev. B **26**, 4199 (1982).
- <sup>17</sup>The distance roughly corresponds to the minimum point of the total energy for the present system (Refs. 8 and 10). The previous slab calculation (Ref. 8) revealed a slight ( $\sim 0.2$  a.u.) outward relaxation of Na atoms with increasing  $\Theta$  which reflects the weakening of the adatom-substrate bonding. However, because of the large extent of Na valence orbitals, the change in the adatom-substrate distance of this order affects quantities such as adatom-dipole moment and adatom DOS only rather little.
- <sup>18</sup>The definition for the adatom DOS coincides with that of Lang and Williams (Refs. 10 and 11) if the sphere radius  $R$  is large enough.
- <sup>19</sup>There is a small downward shift of the peak position with increasing  $\Theta$ , since the peak corresponds to a strongly outward polarized orbital which can feel the lowering of the electrostatic potential in the vacuum side to some extent. However, one cannot expect a depolarization shift for the states below  $\epsilon_F$  which polarize toward the interface side.
- <sup>20</sup>The electron wave function corresponding to the main peak has a node in the Na-jellium interface.